

Direct diode-pumped Kerr-lens mode-locked Ti:sapphire laser

Charles G. Durfee^{1,*}, Tristan Storz,¹ Jonathan Garlick,^{1,2} Steven Hill,¹
Jeff A. Squier,¹ Matthew Kirchner,² Greg Taft,² Kevin Shea,²
Henry Kapteyn,^{2,4} Margaret Murnane,^{2,4} and Sterling Backus^{2,3}

¹*Department of Physics, Colorado School of Mines, Golden, Colorado 80401, USA*

²*KMLabs Inc., Research and Development Department,
1855 S 57th Ct, Boulder, Colorado 80301, USA*

³*Colorado State University, Department of Electrical and Computer Engineering, Ft. Collins,
Colorado 80523, USA*

⁴*JILA, University of Colorado, Department of Physics and NIST, Boulder, Colorado 80309,
USA*

[*cdurfee@mines.edu](mailto:cdurfee@mines.edu)

Abstract: We describe a Ti:sapphire laser pumped directly with a pair of 1.2W 445nm laser diodes. With over 30mW average power at 800 nm and a measured pulsewidth of 15fs, Kerr-lens-modelocked pulses are available with dramatically decreased pump cost. We propose a simple model to explain the observed highly stable Kerr-lens modelocking in spite of the fact that both the mode-locked and continuous-wave modes are smaller than the pump mode in the crystal.

© 2012 Optical Society of America

OCIS codes: (320.7160) Ultrafast optics; (140.3590) Lasers, titanium; (140.7090) Ultrafast lasers.

References and links

1. P. F. Moulton, "Spectroscopic and laser characteristics of Ti:Al₂O₃," *J. Opt. Soc. Am. B* **3**, 125–133 (1986).
2. D. E. Spence, P. N. Kean, and W. Sibbett, "60-fsec pulse generation from a self-mode-locked Ti:sapphire laser," *Opt. Lett.* **16**, 42–44 (1991).
3. B. Resan, E. Coadou, S. Petersen, and A. Thomas, "Ultrashort pulse Ti:sapphire oscillators pumped by optically pumped semiconductor (OPS) pump lasers," *Proc. SPIE* **6871**, 687116–687118 (2008).
4. A. Müller, O. Jensen, A. Unterhuber, T. Le, A. Stingl, K. Hasler, B. Sumpf, G. Erbert, P. Andersen, and P. Petersen, "Frequency-doubled DBR-tapered diode laser for direct pumping of Ti:sapphire lasers generating sub-20 fs pulses," *Opt. Express* **19**, 12156–12163 (2011).
5. G. K. Samanta, S. Chaitanya Kumar, K. Devi, and M. Ebrahim-Zadeh, "High-power, continuous-wave Ti:sapphire laser pumped by fiber-laser green source at 532nm," *Opt. Laser Eng.* **50**, 215–219 (2012).
6. M. Dymott and A. Ferguson, "Self-mode-locked diode-pumped Cr:LiSAF laser," *Opt. Lett.* **19**, 1988–1990 (1994).
7. P. Wagenblast, R. Ell, U. Morgner, F. Grawert, and F. Kärtner, "Diode-pumped 10-fs Cr³⁺:LiCAF laser," *Opt. Lett.* **28**, 1713–1715 (2003).
8. U. Demirbas, M. Schmalz, B. Sumpf, G. Erbert, G. Petrich, L. Kolodziejski, J. Fujimoto, F. Kärtner, and A. Leitenstorfer, "Femtosecond Cr:LiSAF and Cr:LiCAF lasers pumped by tapered diode lasers," *Opt. Express* **19**, 20444–20461 (2011).
9. C. Honninger, R. Paschotta, M. Graf, F. Morier-Genoud, G. Zhang, M. Moser, S. Biswal, J. Nees, A. Braun, and G. Mourou, "Ultrafast ytterbium-doped bulk lasers and laser amplifiers," *Appl. Phys. B* **69**, 3–17 (1999).
10. S. Naumov, E. Sorokin, and I. T. Sorokina, "Directly diode-pumped Kerr-lens mode-locked Cr⁴⁺:YAG laser," *Opt. Lett.* **29**, 1276–1278 (2004).
11. K. Paschke, B. Sumpf, and F. Dittmar, "Nearly diffraction limited 980-nm tapered diode lasers with an output power of 7.7 W," *IEEE J. Sel. Top. Quantum Electron.* **11**, 1223–1227(2005).
12. S. Nakamura, M. Senoh, S.-i. Nagahama, N. Iwasa, T. Matsushita, and T. Mukai, "Blue InGaN-based laser diodes with an emission wavelength of 450 nm," *Appl. Phys. Lett.* **76**, 22–24 (2000).

13. P. Roth, A. Maclean, D. Burns, and A. Kemp, "Directly diode-laser-pumped Ti:sapphire laser," *Opt. Lett.* **34**, 3334–3336 (2009).
14. P. Roth, A. Maclean, D. Burns, and A. Kemp, "Direct diode-laser pumping of a mode-locked Ti:sapphire laser," *Opt. Lett.* **36**, 304–306 (2011).
15. M. T. Asaki, C.-P. Huang, D. Garvey, J. Zhou, H. C. Kapteyn, and M. M. Murnane, "Generation of 11-fs pulses from a self-mode-locked Ti:sapphire laser," *Opt. Lett.* **18**, 977–979 (1993).
16. K. Read, F. Blonigen, N. Riccielli, M. Murnane, and H. Kapteyn, "Low-threshold operation of an ultrashort-pulse mode-locked Ti:sapphire laser," *Opt. Lett.* **21**, 489–491 (1996).
17. A. Kowalevicz Jr, T. Schibli, F. Kärtner, and J. Fujimoto, "Ultralow-threshold Kerr-lens mode-locked Ti:Al₂O₃ laser," *Opt. Lett.* **27**, 2037–2039 (2002).
18. M. Piché and F. Salin, "Self-mode locking of solid-state lasers without apertures," *Opt. Lett.* **18**, 1041–1043 (1993).
19. S. Namiki, E. Ippen, H. Haus, and C. Yu, "Energy rate equations for mode-locked lasers," *J. Opt. Soc. Am. B* **14**, 2099–2111 (1997).
20. P. Moulton, "An investigation of the Co:MgF₂ laser system," *IEEE J. Quantum Electron.* **21**, 1582–1595 (1985).
21. O. Svelto, *Principles of Lasers* (Springer Verlag, 2009).
22. A. Alfrey, "Modeling of longitudinally pumped CW Ti:Sapphire laser oscillators," *IEEE J. Quantum Electron.* **25**, 760–766 (1989).

1. Introduction

Titanium-doped sapphire is an excellent and widely-used gain medium, with an active ion which has a large bandwidth in a host crystal that is hard and has high thermal conductivity [1]. The high saturation intensity requires longitudinal laser pumping by a high-brightness beam mode tightly focused to approximately 30 μ m in the crystal. The first Ti:sapphire CW and ultrafast mode-locked lasers were pumped with Argon-ion lasers [2] (488nm, 515nm) near the peak of the absorption curve for the Ti³⁺ ion. Currently, expensive Nd:YVO₄ intracavity doubled pump lasers (that cost \approx \$20k for 3W output) are typically used to pump Ti:sapphire oscillators. Other alternative pumping sources for Ti:sapphire include optically-pumped semiconductor lasers [3], frequency-doubled DBR-tapered diode lasers [4] and frequency-doubled Yb fiber lasers [5]. The low cost of direct diode pumping has led to the investigation of other ultrafast laser materials, such as Cr:LiSAF [6–8], Yb-doped materials [9], and other gain media farther in the infrared [10]. A Cr:LiSAF laser was pumped by two collinear broad stripe laser diodes by Wagenblast *et al* [7]. With an emitting area of 100 μ m x 1 μ m, the highly aberrated slow axis was difficult to focus tightly, leading to a focal spot size aspect ratio of approximately 3.5:1, and a short depth of focus of 0.8mm. However, by using the high beam quality of a tapered laser diode [11], the output power of the Cr:LiSAF laser was dramatically improved [8].

Although high-power laser diodes very near the peak absorption of Ti³⁺ at 500nm are not yet available, the recent development of 445 nm diodes [12] at high power (over 1W) has opened up the possibility of directly diode-pumping Ti:sapphire oscillators. These diode lasers have an emitter area of approximately 15 μ m x 1 μ m. Although frequency-doubled diode lasers can be used to pump Ti:sapphire lasers [4], the simplicity, robustness and cost savings of direct diode pumping is attractive: 445nm diodes can be less than US\$400 for a complete double laser package producing 2.2 W. Recently, work by the University of Strathclyde in Scotland, demonstrated the direct diode pumping of a Ti:sapphire laser oscillator [13], and subsequent modelocking by use of intracavity prisms and a saturable Bragg reflector (SBR) [14]. In this paper, we report the sustained Kerr lens modelocking of a Ti:sapphire oscillator using 2.2 W of 445 nm laser diodes and intracavity prisms. In our system, there is no SBR or SESAM to assist in modelocking. Moreover, we do not observe parasitic losses that were seen by Roth *et al* and attributed to the short pumping wavelength [13]. Direct diode-pumped Ti:sapphire lasers have great promise to increase reliability and portability for a new generation of ultrafast laser systems.

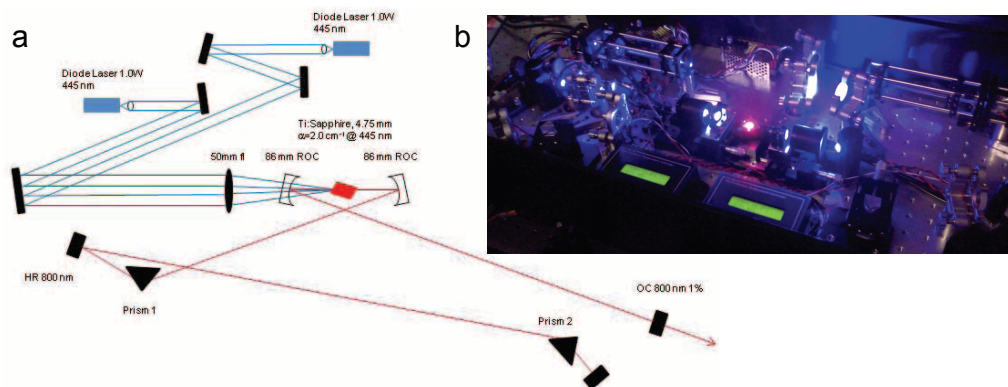


Fig. 1. (a) Layout for diode-pumping Ti:sapphire laser with two beams. (b) Photograph of laser in operation.

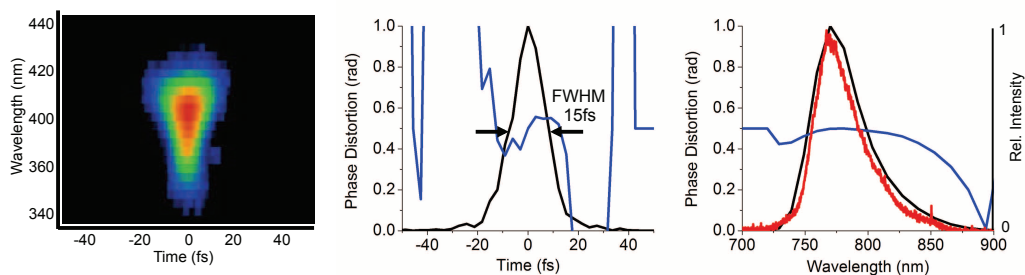


Fig. 2. (a) Frog trace. (b) Deconvolved temporal intensity and phase (black, blue). (c) Deconvolved spectral intensity and phase (black, blue). Separately measured spectrum (red).

2. Laser configuration and results

2.1. Oscillator design and pumping system

The layout of the oscillator (Fig. 1(a)) is based on a standard commercial KMLabs oscillator [15]. It was modified to run at low pumping threshold by using slightly shorter focal length curved mirrors (86 mm ROC compared to 100mm), and 1% output coupling mirror centered at 800nm. The Brewster-angle Ti:sapphire crystal is 4.75 mm thick with an absorption coefficient of $\alpha = 3\text{cm}^{-1}$ at 514nm and $\alpha = 2\text{cm}^{-1}$ at 445nm, giving 60% absorption of the pump light. The crystal has a figure of merit of greater than 200. The laser is pumped by two 1.2 W 445 nm laser diodes that are polarized along the long axis of the diode output facet. For both diodes, this long facet axis was oriented in the horizontal (x) direction, so that the beam diverged faster in the vertical (y) direction. To avoid pushing the diode lasers to their rated limit, the laser diodes were operated at 1W each, with 1.8W delivered through all optics to the crystal. The diode lasers were collimated by aspheric lenses followed by a 3:1 cylindrical telescope applied to the slow axis. We observed that the fast and slow axes of the diode beam, when collimated only with the aspheric lens, focused to different planes, so the cylindrical telescope was adjusted to place the two beam waists at the same plane. The diodes were TEC-cooled to stabilize the output power. For these diodes we observed very little temperature tuning of the wavelength. The intracavity prisms used for dispersion compensation are fused silica, and are placed 650

mm apart.

Aside from the slightly smaller mirror radius and the low output coupling, the laser design is conventional. The most important factor for stable operation is to get as much pump power absorbed in a sufficiently small spot in the crystal. The laser cavity was first optimized using a beam from a frequency-doubled Nd:YVO₄ laser. In initial experiments, we used 6mm focal length aspheric lenses to collimate the pump beams and focused them with 50 mm lenses onto the Ti:sapphire crystal from both sides. Slight angular detuning of the beams was important to avoid feedback from one diode into the next. Later we developed a more robust configuration in which we used 4mm aspheric lenses and directed them side-by-side along the horizontal direction into the 50mm pump lens from one side of the crystal. The blue pump beams were reflected off a dichroic mirror through which the 532nm pump beam passed. This allowed us to keep the laser above threshold while optimizing each blue pump beam individually.

Kerr lens modelocking is initiated by introducing an intensity spike by rapidly moving one of the prisms. Using counter-propagating pump beams we were able to obtain approximately 40mW of mode-locked output power; pumping from the same side, 34mW. When pumping with the 532nm beam alone, we are able to initiate and sustain modelocking at a pump power of 500mW, with an output power of 30mW. This is comparable to early work on low-threshold Ti:sapphire lasers [16], though not quite as low as seen by Kowalevicz et al. [17] or Roth et al. [14]. We directed the output beam through a pair of chirped mirrors to compensate for the dispersion of the output coupler, then sent the beam into a scanning frequency-resolved optical gating (FROG) pulse measurement system. Figure 2 shows the FROG trace along with the deconvolved time- and wavelength-domain intensities and phases. As is typical with these lasers, the spectral shape is controlled by the prism and the curved mirror positioning. We obtained a pulse with 15fs full-width at half-maximum duration. Temporal smearing from the beam crossing angle in the FROG device may lead to measured duration that is 1-2fs longer than the actual duration. The output beam quality is excellent, with a measured M^2 value that is very close to 1.0 (Fig. 3(a) and 3(b)). When the modelocking is interrupted, we find that the CW power is lower than the mode-locked power by a factor of 3. This strong preference of the laser for Kerr-lens modelocking leads to high long-term stability. The power output of the blue diode-pumped Ti:sapphire (measured with a diode power meter) is compared to a similar commercial laser (KMLabs Griffin) pumped with 532nm, and measured with a pyroelectric meter (Fig. 3(c)). When covered in a box, the DDPTS laser stays mode-locked indefinitely with a measured RMS noise of 1.3%. We do not observe the photo-darkening described in earlier work by Roth [13].

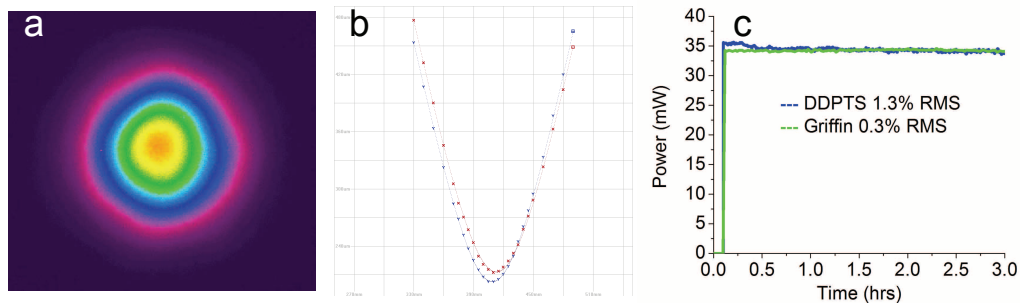


Fig. 3. (a) Output beam profile. (b) X and Y beam width through focus. (c) Output power vs time from start up comparing DDPTS (blue) with Ti:sapphire laser pumped with a diode-pumped Nd:vanadate laser (green).

To provide more information about the pump-laser mode overlap, we collected pump and laser light that leaked through the curved mirror opposite the pump mirror (see Fig. 1) with a 50mm focal length lens. After propagation of 1m, the beams were directed into the lens ($f = 300\text{mm}$) of an M^2 beam profiler. We measured the variation of the beam size through the focus for the pump beams together, the IR mode-locked beam, and the IR CW beam. By performing a ray trace of the optics, we mapped the measured spot sizes back to the crystal. The plots of the beam sizes are shown in Fig. 4(a), where the stretching due to the Brewster cut of the crystal in the x -direction is ignored. Some astigmatism in the x - and y -profiles is seen, which is expected since the output beam reflects from the tilted curved mirror before leaving the laser. Interestingly, there is a shift in the axial position of the waist when the modelocking of the laser is interrupted and the laser operates in the continuous wave regime. The beam profile of the combined blue pump beams is shown in Fig. 4(b). The beam profile is narrower in the y -direction as expected for the fast axis, with a FWHM of approximately $24\mu\text{m}$, which is somewhat larger than the infrared mode. There is a substantial fraction of the pump power that is in a tail in the y -direction. If this can be improved with better quality optics, the output power of the oscillator would increase. The mode size of the pump is seen to vary little through the length of the crystal in the vertical direction, but owing to the crossed pump beams in the horizontal direction, the size in the x -direction increases by approximately 50% at either end of the crystal relative to its value in the center.

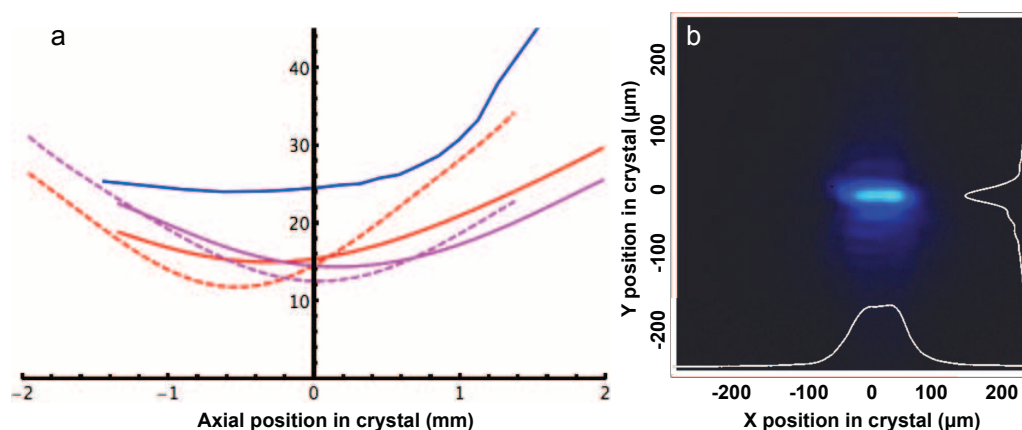


Fig. 4. (a) Variation of the infrared beam and vertical pump mode beam sizes (FWHM) with axial distance within the crystal. Red: CW mode, Purple: mode-locked mode, Blue: vertical (y) pump mode; Dashed: x cross-section, Solid: y cross-section. Due to chromatic aberration in the imaging optics, the exact axial alignment of the blue and IR waists is uncertain. (b) Image of the two crossed pump beams with transverse scale corresponding to size in the crystal. FWHM in the x -direction is approximately $80\mu\text{m}$, in the y -direction $24\mu\text{m}$.

3. Discussion

The conventional understanding of soft-aperture Kerr-lens modelocking [18, 19] is that the non-linearity allows the mode in the crystal to be smaller when mode-locked than CW. When mode-locked the beam in the crystal matches the pump mode for best power output, while the CW mode is bigger than the pump which therefore reduces the output power. For lasers directly pumped by diode lasers, the challenge is the low brightness of the pump source. In this diode-

pumped Ti:sapphire laser, both the CW and mode-locked beams are smaller than the pump mode in the horizontal direction, and are similar to the pump mode in the vertical direction. In the future we plan a more detailed study of the pump/IR mode overlap; at present we make some observations about factors that can contribute to the observed efficiency of the Kerr lens modelocking in this laser. First, while the pump mode size is clearly larger than the IR mode size in the x -direction, they are much more closely matched in the y -direction. Therefore if the transition from mode-locked to CW involves a stretching of the mode in the vertical direction, it could lead to a strong difference in the gain [10]. In our case, there does not appear to be a strong change in the degree of astigmatism, so while this mechanism may play a role, it may not be the dominant effect. Second, it is clear that there is a measurable shift in the waist position between CW and ML operation. This can lead to a difference in the mode overlap when integrated across the crystal.

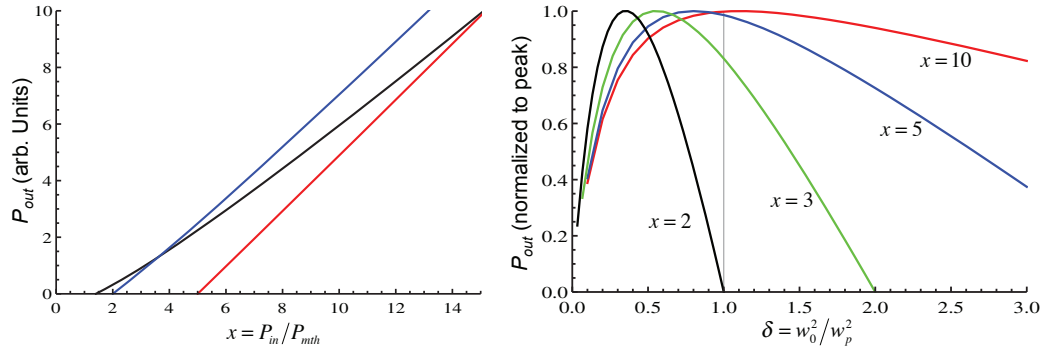


Fig. 5. (a) Output power vs input power normalized to the minimum threshold power (P_{mth}) where the laser mode size is negligibly small. Lines correspond to different values of $\delta = w_0^2/w_p^2$: Black: $\delta = 0.4$, Blue: $\delta = 1$, Red: $\delta = 4$ (b) Output power as a function of δ for several values of the pump rate.

Finally, in Fig. 5, we offer a simple picture of how KLM can be preferred even when the pumped area is larger than both of the ML and CW laser modes. Our simple model, based on one by Moulton [20] and Svelto [21], accounts for the spatial dependence of the gain and the laser mode to calculate the relation of output power to input power for a longitudinally pumped laser with different size Gaussian pump and laser modes (radii w_p and w_0 , respectively). In a later paper, we will develop a more complete consideration of the mode-gain overlap that includes longitudinal effects and absorption at the lasing wavelength [22], but our simple model illustrates the essence of the argument.

The threshold for lasing depends only on the gain in the crystal vs. the system losses. Since the gain is highest in the center of the pump mode, the threshold will be the lowest in the limit of small mode size. This minimum threshold pump power is

$$P_{mth} = \frac{\gamma}{\eta_p} \frac{h\nu_p}{\tau} \frac{\pi w_p^2}{2\sigma_e} \quad (1)$$

Here, γ is the logarithmic loss, η_p is the pump efficiency, $h\nu_p$ is the pump photon energy, and τ and σ_e are the fluorescence lifetime and the stimulated emission cross-section, respectively. While the pump threshold is lower for small laser mode, the slope efficiency increases with the laser mode, leveling off when the laser mode size is equal to the pump mode size. In Fig. 5, x is the ratio of the input pump power to the minimum threshold power ($x = P_{in}/P_{mth}$). As can

be seen in the x -intercept of Fig. 5(a), the actual pump threshold increases with larger w_0 . A straightforward calculation of the mode-averaged gain shows that $P_{th}(w_0) = P_{mth}(1 + \delta)$ where $\delta = w_0^2/w_p^2$. On the other hand, it can be seen that the slope efficiency is low for small w_0 (black line), while the slope efficiency is nearly the same for $\delta = 1$ as it is for $\delta = 4$. The end result is that for operation near the minimum threshold, it is possible to obtain higher output power for $\delta < 1$ than for $\delta = 1$.

Figure 5(b) shows how the output power varies with δ for different pump powers. Lasers are normally operated with $x \gg 1$. Consider, for example, the red curve in Fig. 5(b) where $x = 10$. The output power maximizes at equal pump and laser mode size ($\delta = 1$). If the mode-locked mode size is near this maximum, operation at CW with a larger mode size will result in lower output power. This is the conventional regime for Kerr-lens modelocking. However, for low pumping power, it can be seen that the maximum output power is at a laser mode size that is smaller than the pump ($\delta < 1$). This results from the strong dependence of the threshold power on laser mode size for low pump power. In our laser, the power discrimination between mode-locked and CW is a factor of 2, showing strong preference for the laser to operate in the mode-locked regime. For a given available pump power and a laser mode size (defined by the cavity), the operational variable is the size of the pump mode. Decreasing w_p leads to an increase both in x and δ , so as we are able to focus our diodes to a smaller spot, we anticipate still higher output power in the mode-locked regime. This simple model only accounts for lowest-order mode overlap in the transverse direction. We are investigating a more complete model [22] that accounts for overlap over the whole crystal volume. For operation near threshold, higher-order modes should be suppressed in spite of the large pump mode volume. We note that relative to a crystal with high absorption efficiency, the gain in the current system is less concentrated at the entrance face of the crystal. This may help in the discrimination against larger and higher-order modes.

4. Conclusion

We believe that this is the first demonstration of stable Kerr lens modelocking, by a direct diode pumped Ti:sapphire laser oscillator. In the previous demonstration of modelocking of a Ti:sapphire laser, [14] which required an SBR to sustain modelocking, the authors reported 12mW of average power in a 114fs pulse. We achieve 34mW of output power in a 15fs pulse without the need for an SBR mirror. We anticipate that with better modematching of the pump beams with the cavity mode, we could increase the output power from 34mW to 100mW. This work opens the door to much more inexpensive and robust femtosecond oscillator, and the potential for cost effective amplifier systems.

Acknowledgments

C. D. and J. S. acknowledge funding support from AFOSR under grant FA9550-10-1-0394. J. S. acknowledges support from NIH grant EB003832. S. B. and J. S. acknowledge funding from an STTR AFOSR FA9550-10-C-0017, and S. B. from a AFRL SBIR FA8650-11-C-2102.